Nanoscale Materials: Exploring the Energy Frontier

Prashant N. Kumta
Department of Materials Science and Engineering,
Biomedical Engineering
Carnegie Mellon University,
Pittsburgh, PA 15213

Need for Energy Storage Systems

- Hybrid Electric Vehicle
- Backup Power Source
- Telecommunication
- Electronic Devices
- Laser
- Military Use
- Particle Accelerator

www.nissandiesel.co.jp

www.hondacorporate.com

www.nissandiesel.co.jp

www.maxwell.com

Nissan Diesel
Sizuki Electric
Power Systems

www.maxwell.com

Potential Energy Storage Systems

- Li-ion Batteries*
- Super-capacitors*
- Direct Methanol Fuel Cells*
- Hydrogen Storage

*Focus of the current presentation

Lithium-Ion Systems: Anodes and Cathodes

Comparison of Battery Energy Density
(gravimetric and volumetric)

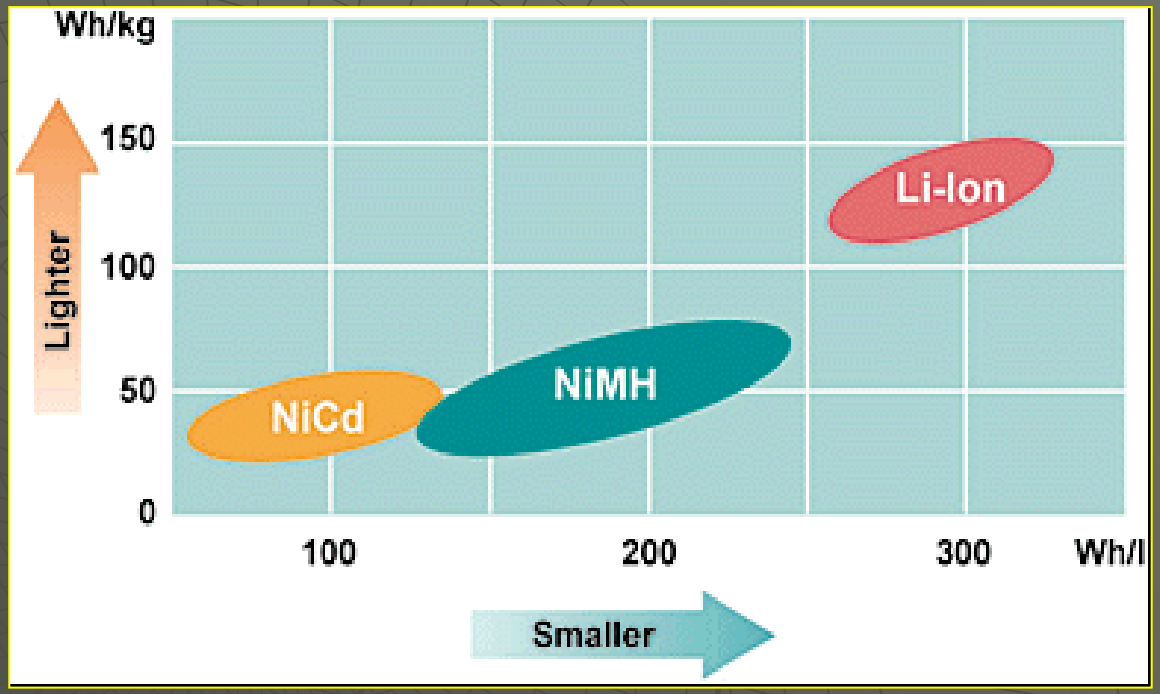

Considerable improvement in area of cathodes with identification of new layered compounds, $LiFePO_4$ and $LiNi_{0.5}Mn_{0.5}O_2$, $LiMn_{1/3}Ni_{1/3}Co_{1/3}O_2$. Improvements in the anode area are still warranted.

Introduction and Background

- **Li-alloy (Li_xM) : Anodes for Li ion cells**
  - Intermetallic phases containing lithium

    $Li_xM \rightleftarrows xLi^+ + xe^- + M$

    (M = Mg, Ca, Al, Si, Ge, Sn, Sb, Bi, Zn, etc)[1]
  - Higher theoretical capacity than graphite

    (LiC_6 : 372 *mAh/g*, 832 *Ah/L*,

    $Li_{22}Sn_5$: 990 *mAh/g*, 14780 *Ah/L*

    $Li_{22}Si_5$: 4000 *mAh/g*, 10997 *Ah/L*)[1, 2]

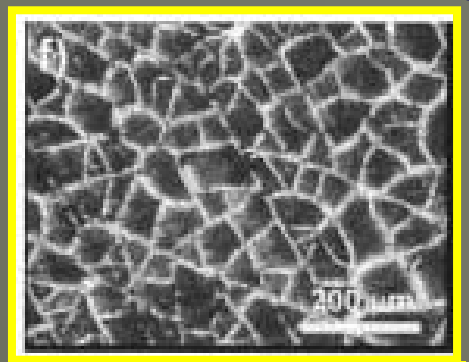

- **Major problems of Li-alloys for use as anodes**
  - Poor reversibility caused by large volume changes

    (Sn: 593%, Si: 412% volume change)
  - Cracking or crumbling during cycling

1. M. Winter & J. O. Besenhard, *Electrochimica Acta*, 1999, 45, 31.
2. B. A. Boukamp & R. A. Huggins, *J. Electrochemical Soc.*, 1981, 128, 729.
3. L.Y. Beaulieu, K.W. Eberman, R.L. Turner, L.J. Krause and J.R. Dahn, *Elect. Sol. St. Lett.* 2001, A137.

Carnegie Mellon ENGINEERING

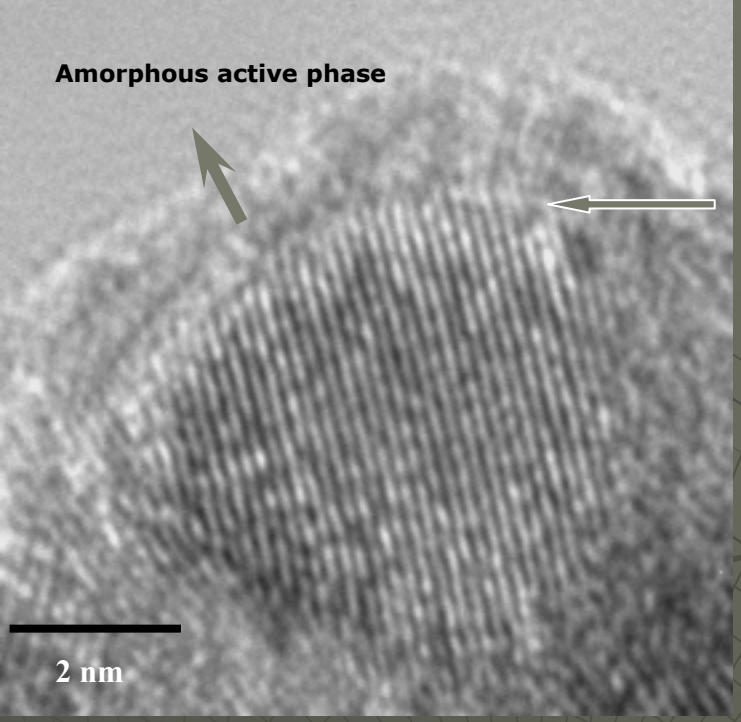

- No secondary phase observed at the interface
→ Si/Transition metal non-oxide system is stable during HEMM.

Nanoscale structure is the key to attaining the high capacity

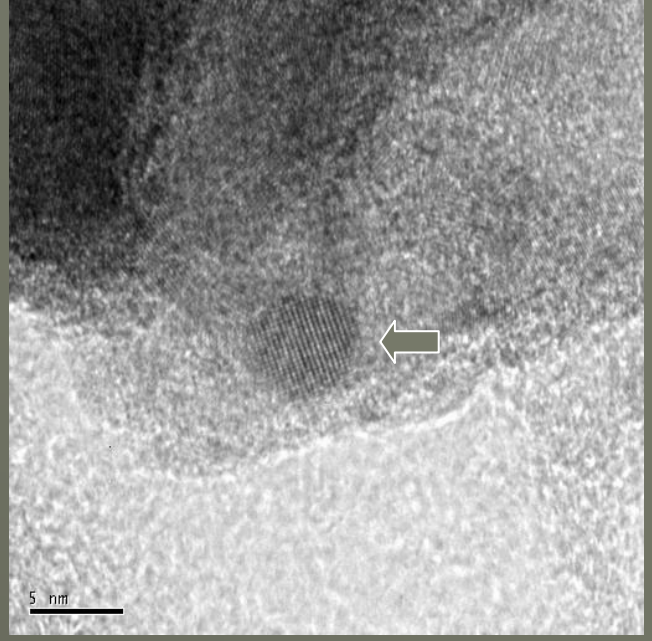

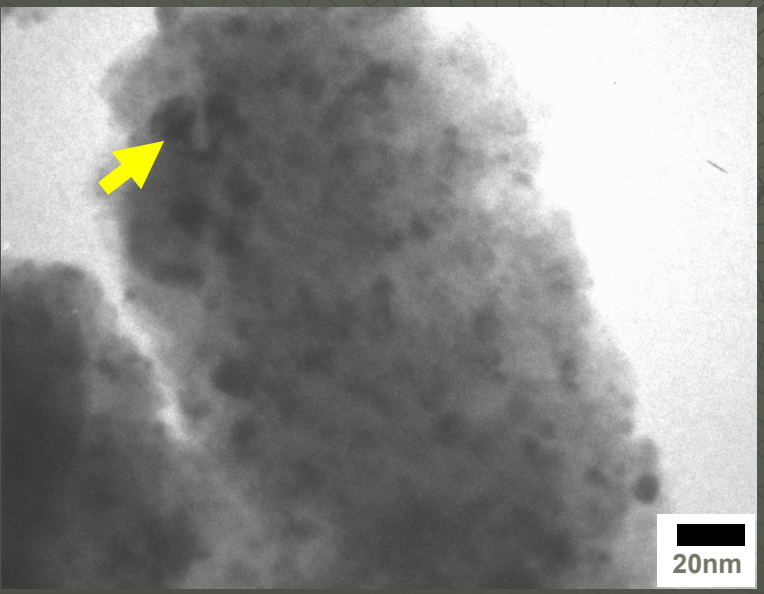

Bright Field

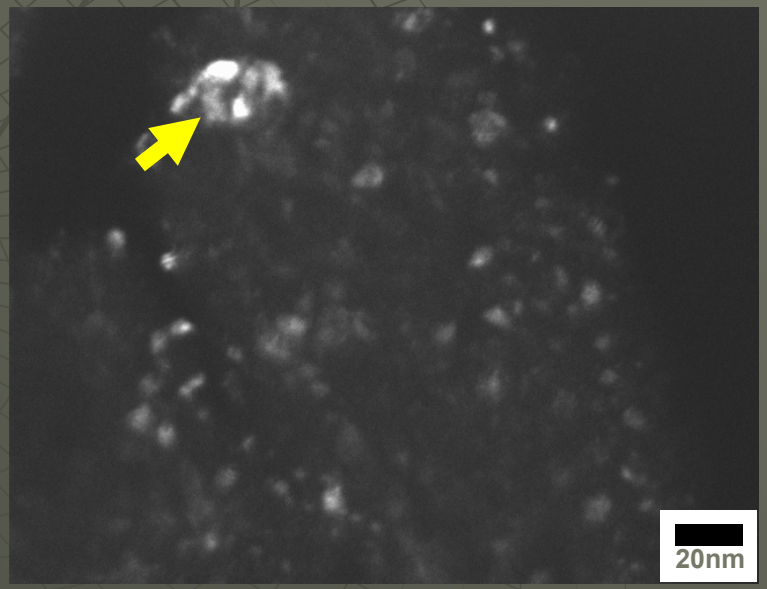

Dark Field

Electrochemical Response(Sn:C=1:1)

(Tetraethyl tin+Ps-resin powder heat-treated at 600 °C for 5h in UHP-Ar, current rate = 100μA/cm²)

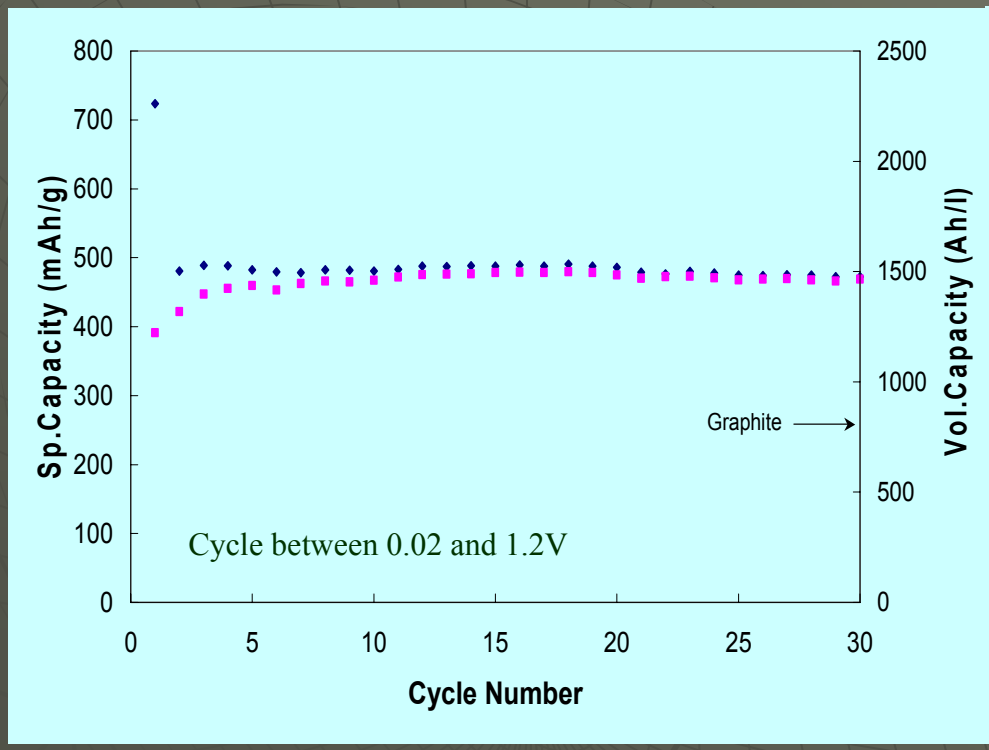

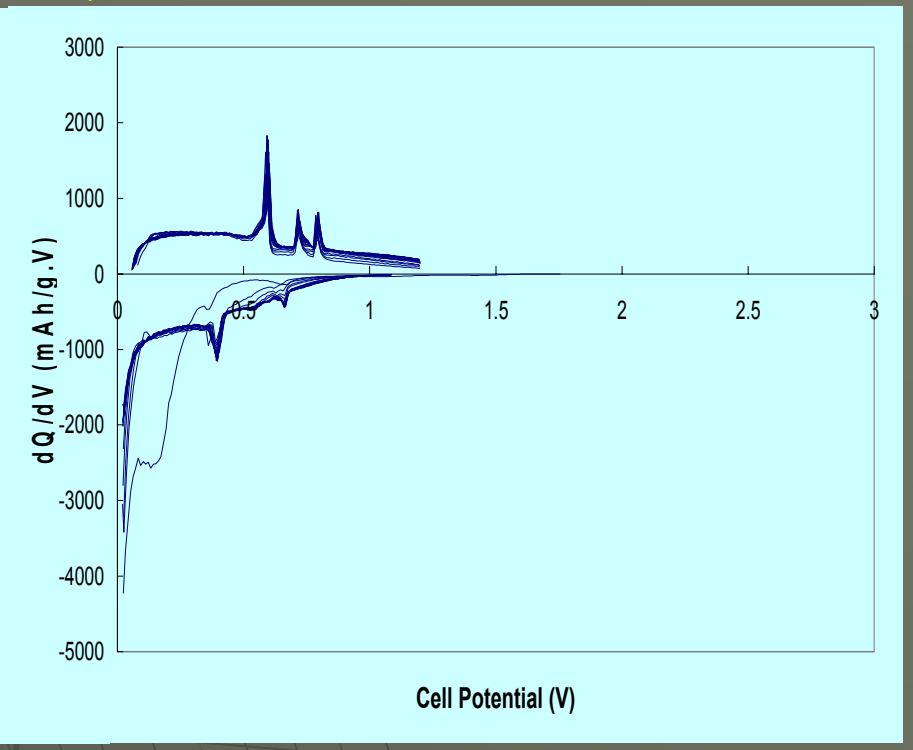

- Theoretical Capacity = 636 mAh/g
- Higher capacity than graphite (~480mAh/g or 1450Ah/l) with stability (0.15%loss/cycle).

HEMM derived Si-C nanocomposites

Nanostructured inactive matrix can endure large volumetric stresses of the active material due to possible superplastic deformation that can provide compressive stresses to accommodate large strains*.

$$\dot{\varepsilon} = \sigma^{n} d^{-p} D_{o} \exp(-Q/RT)$$

*** M.J. Mayo, Nanostructured Materials, Vol. 9 (1997) 717**

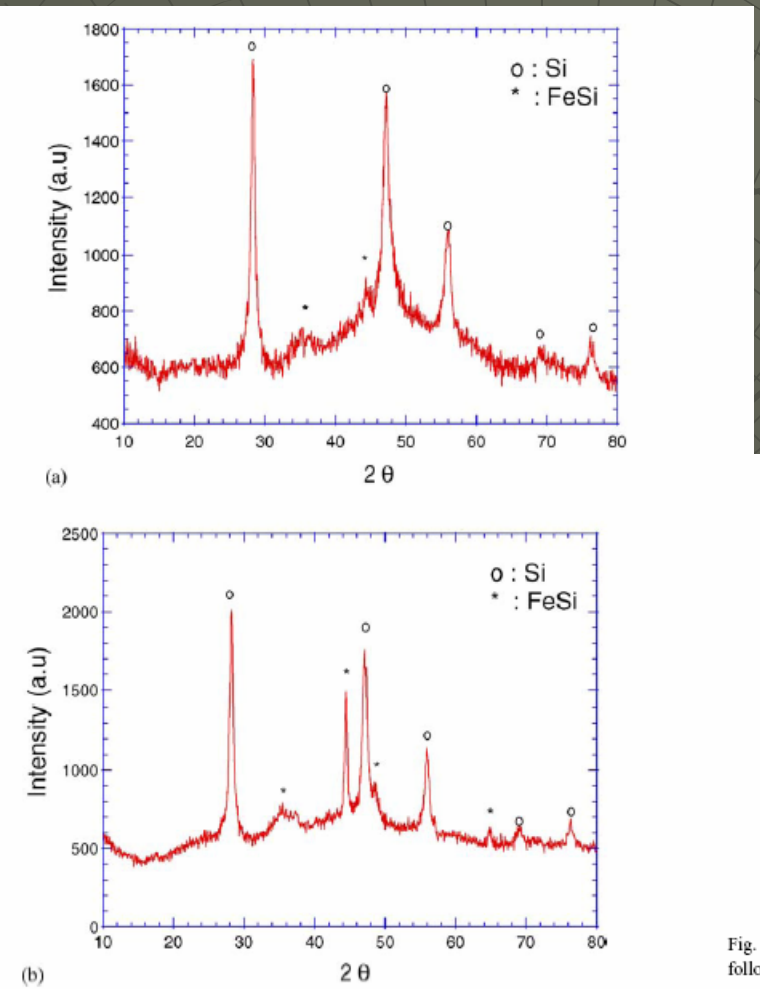

Fig. 2. (a) XRD patterns of the nanocomposite containing Si:C = 1:2 obtained after milling for 12 + 12 h (before heat-treatment), and (b) after subsequent heat-treatment in UHP-Ar/H_2 (5%) for 5 h at 800 °C.

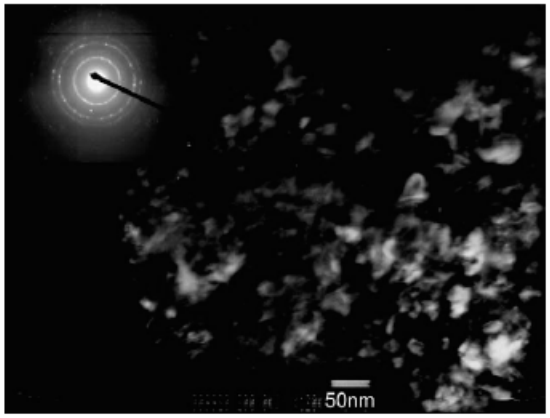

Fig. 3. The dark field image and the SADP of the nanocomposite containing Si:C = 1:2 obtained after milling for 12 + 12 h followed by subsequent heat-treatment in UHP-Ar/H_2 (5%) for 5 h at 800 °C (the SADP is shown in the inset has been collected with camera length = 80 cm, reduced to 33% of its original size).

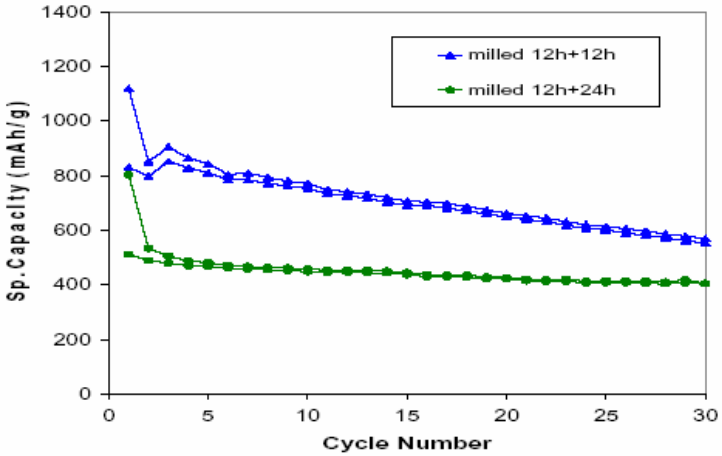

Fig. 4. Capacity as a function of cycle number for Si/C nanocomposites containing 33 mol.% Si obtained after milling for 12 + 12 h and 12 + 24 h followed by subsequent heat-treatment in UHP-Ar/H_2 (5%) for 5 h at 800 °C (current rate: 100 μA/cm^2, potential: 0.02–1.2 V).

XTEM of sputter deposited Si film (250 nm as-deposited film)

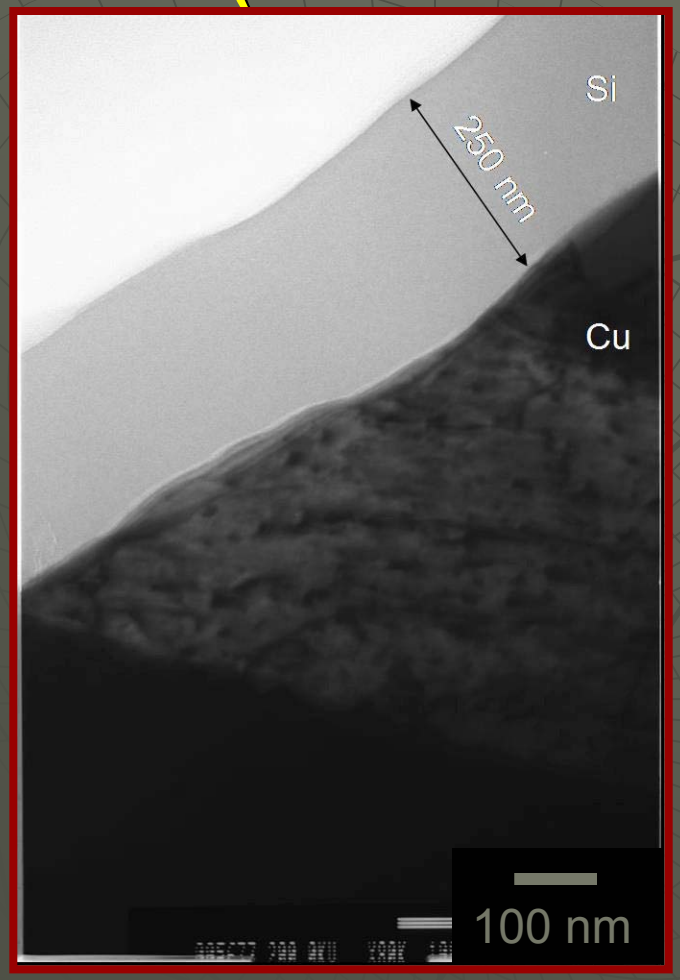

Conventional XTEM

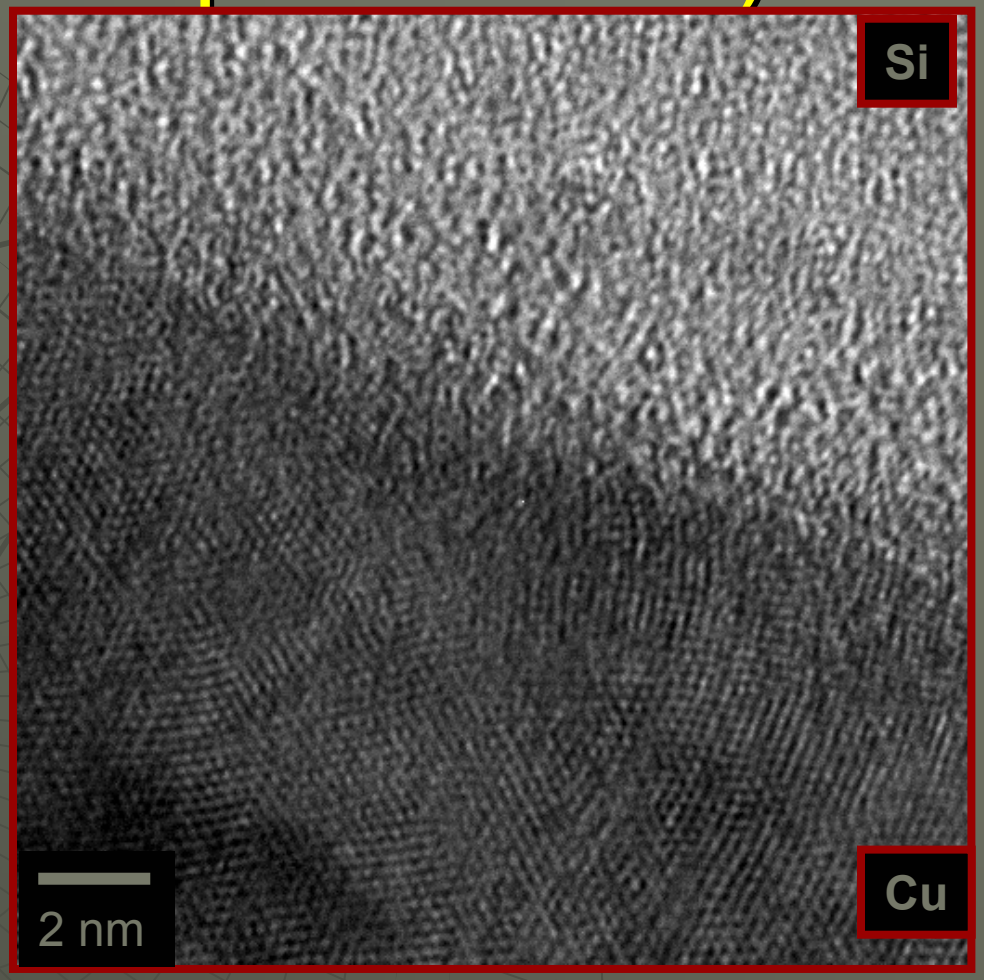

High Resolution XTEM

Galvanostatic Cycling of 250 nm Si Thin Film (C/2.5 and 2C rates)

Also note low irreversible loss ~14% and 0.1 % loss per cycle.

Increase of capacity with cycle # for the 2C sample may be due to kinetic limitation of the amorphous Si sample in the initial cycles, which is mitigated gradually in later cycles by morphological changes in the electrode, decreasing the effective diffusion distance for the lithium ions from the electrolyte.

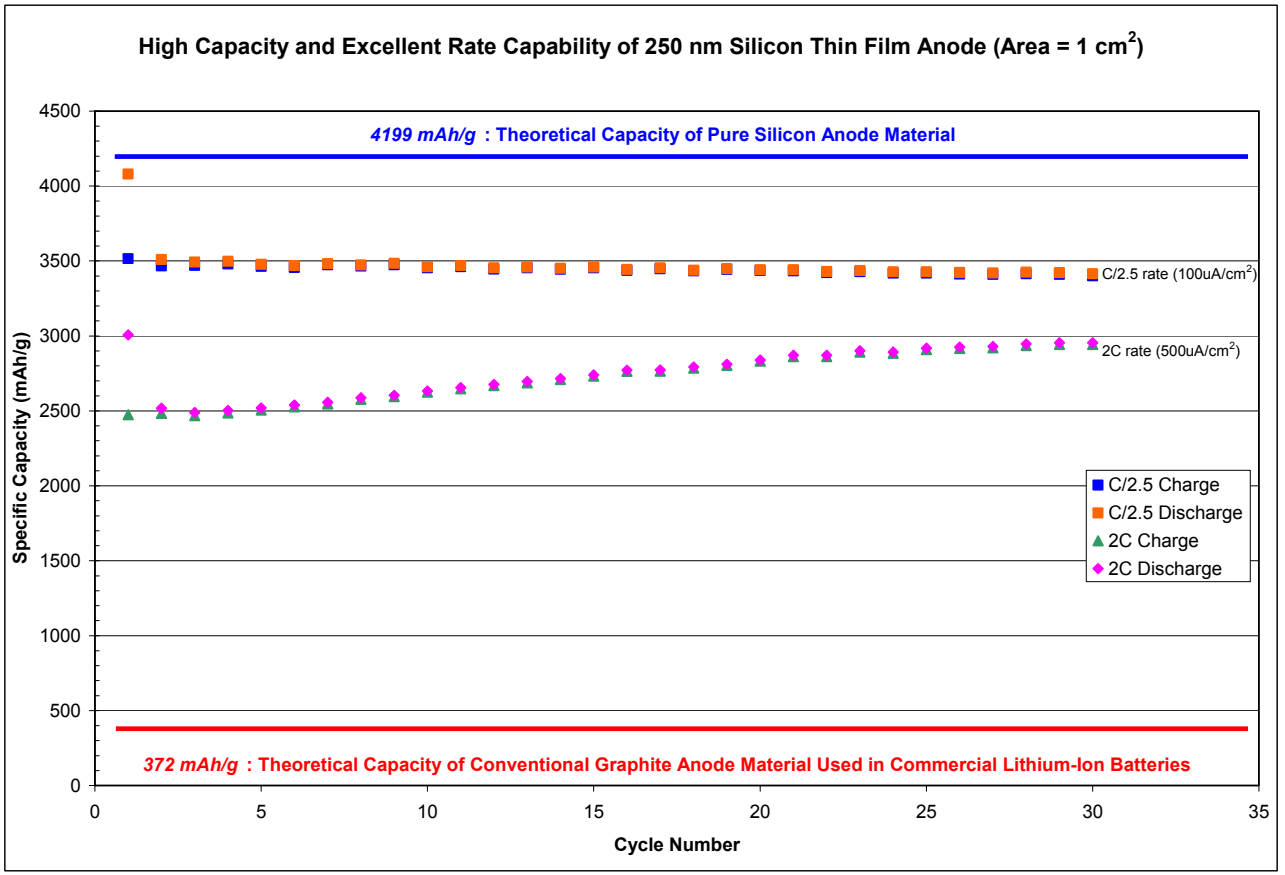

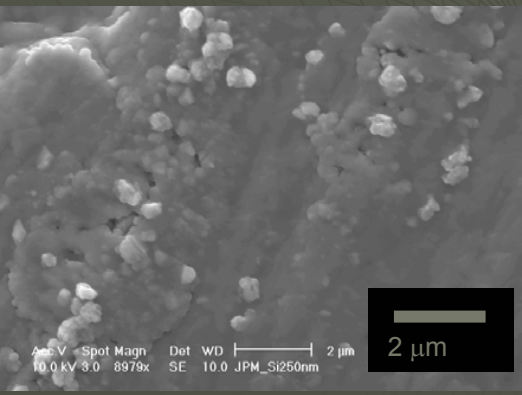

As-Deposited

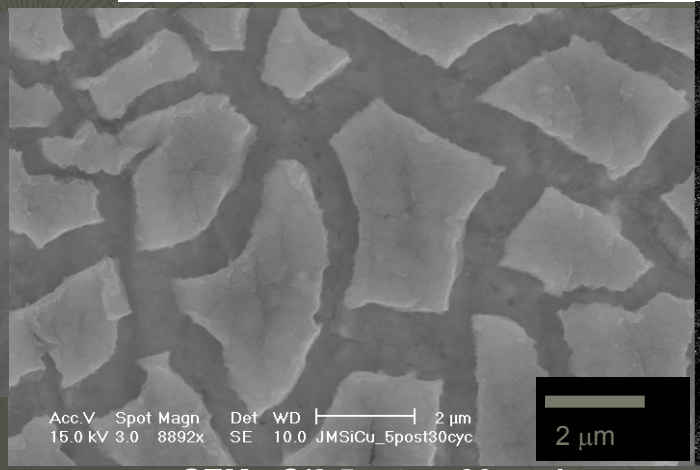

SEM : C/2.5 rate – 30 cycles

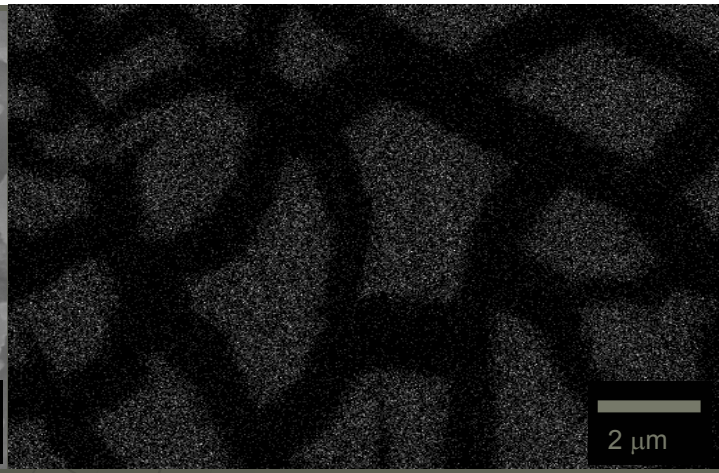

Si EDAX : C/2.5 rate – 30 cycles

Multilayer Film Schematic

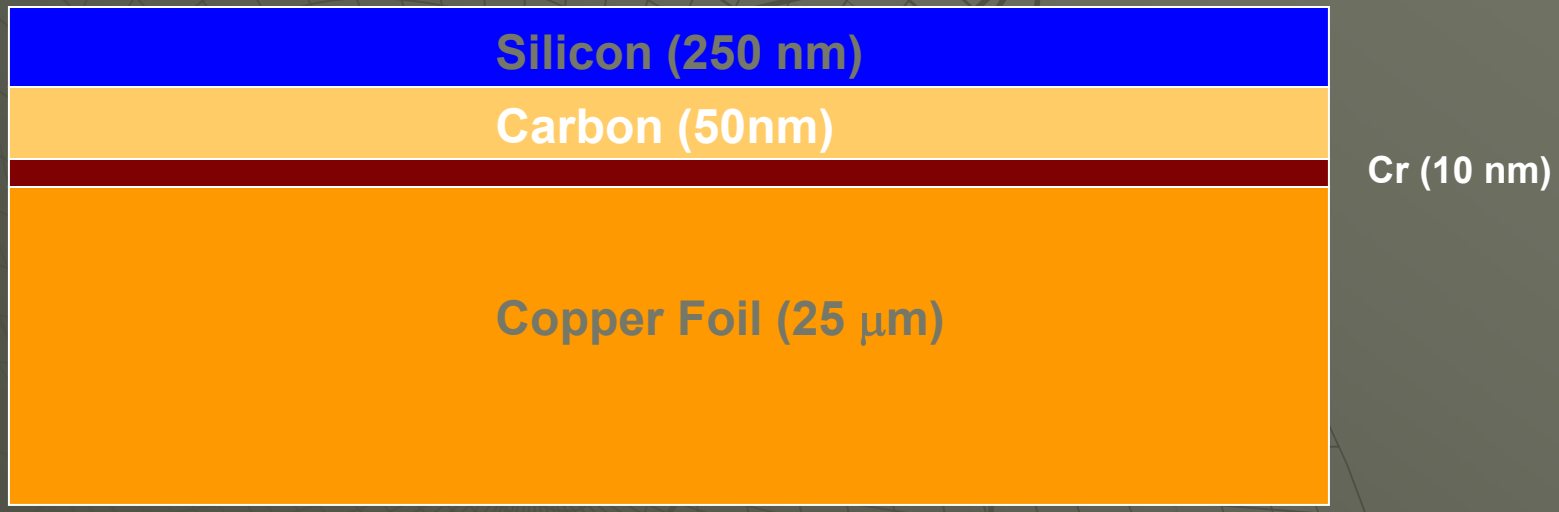

Note: Drawing not to scale

Note: E_{carbon} ~ 50 – 500 GPa

Cycling of Multilayer Film, C/2.5 rate

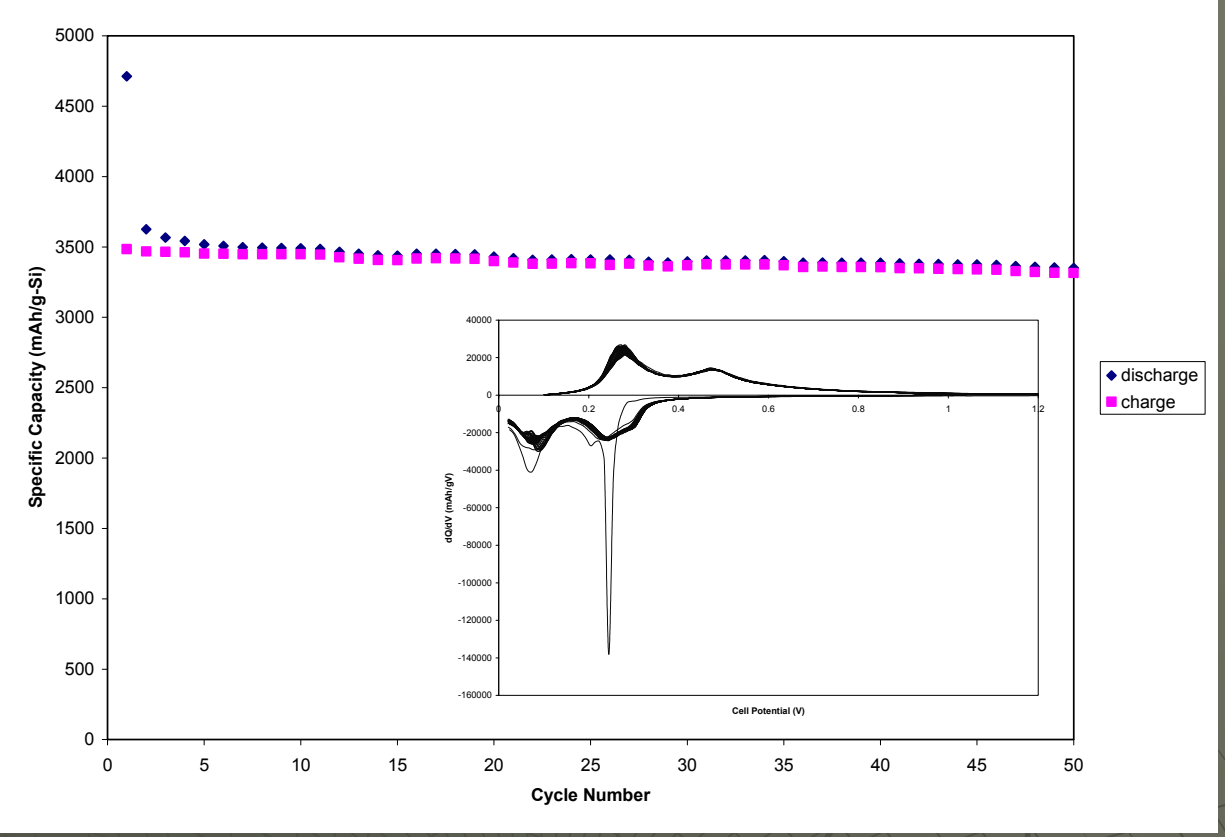

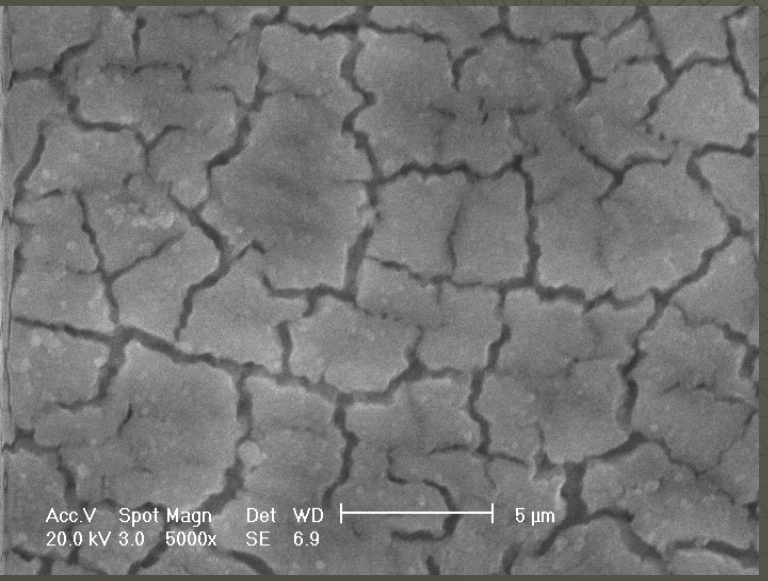

SEM image of a 500°C-4h annealed 250 nm Si/50nm C/10 nm Cr/Cu multilayer thin film cycled at 0.4 C after 75 cycles, 5000x.

Interface dynamics control of the nanoscale films is the key to improved electrochemical performance

Supercapacitors: Potential Energy Storage Systems

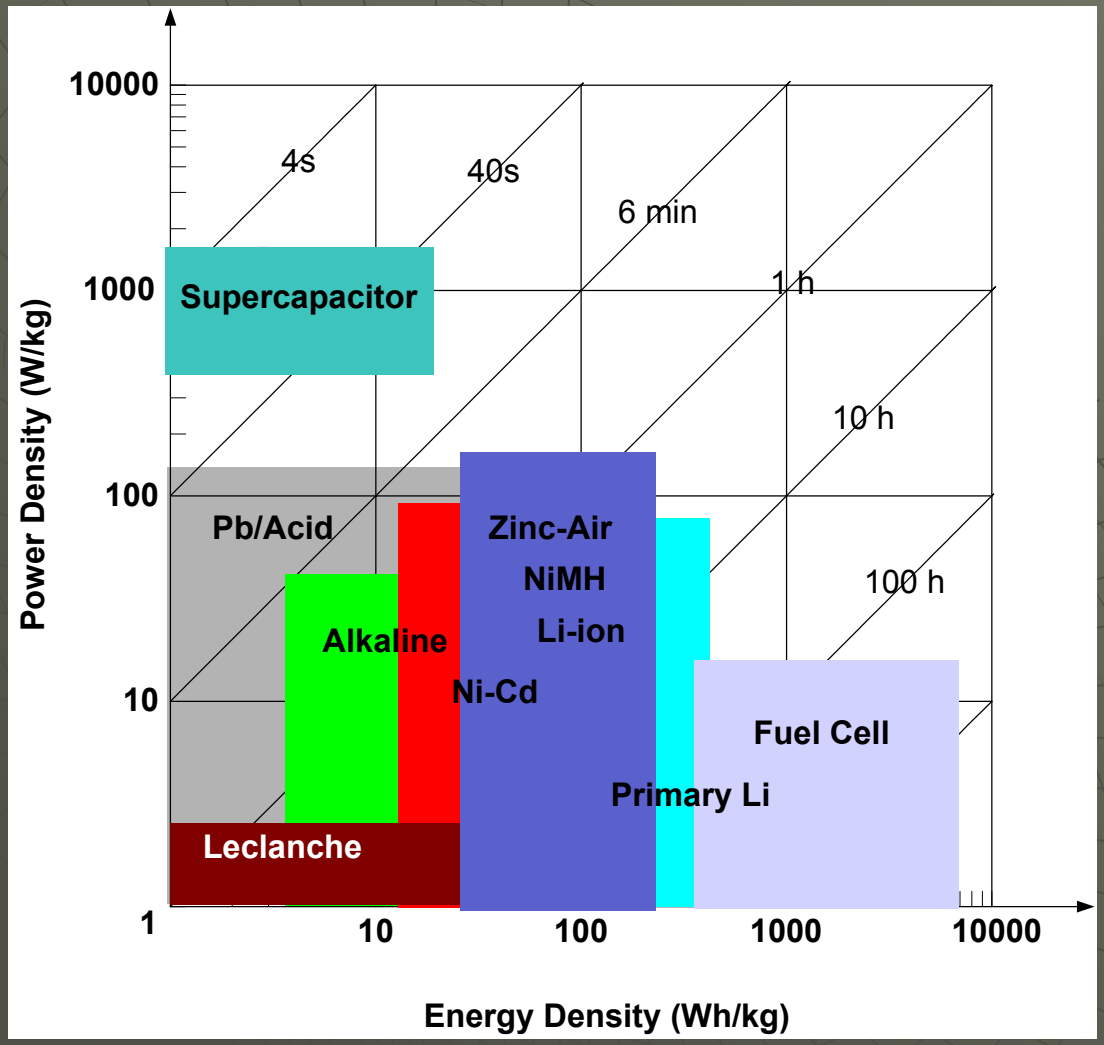

Ragone Plot

- Electrochemical Capacitor

  "Ultracapacitor"
  "Supercapacitor"

- Primary Battery
  - Leclanche
  - Primary Li
  - Alkaline

- Secondary Battery
  - Pb/Acid
  - Zinc-Air
  - Ni-Cd
  - NiMH
  - Li-ion

- Fuel Cell

Electrical Double Layer (EDL)

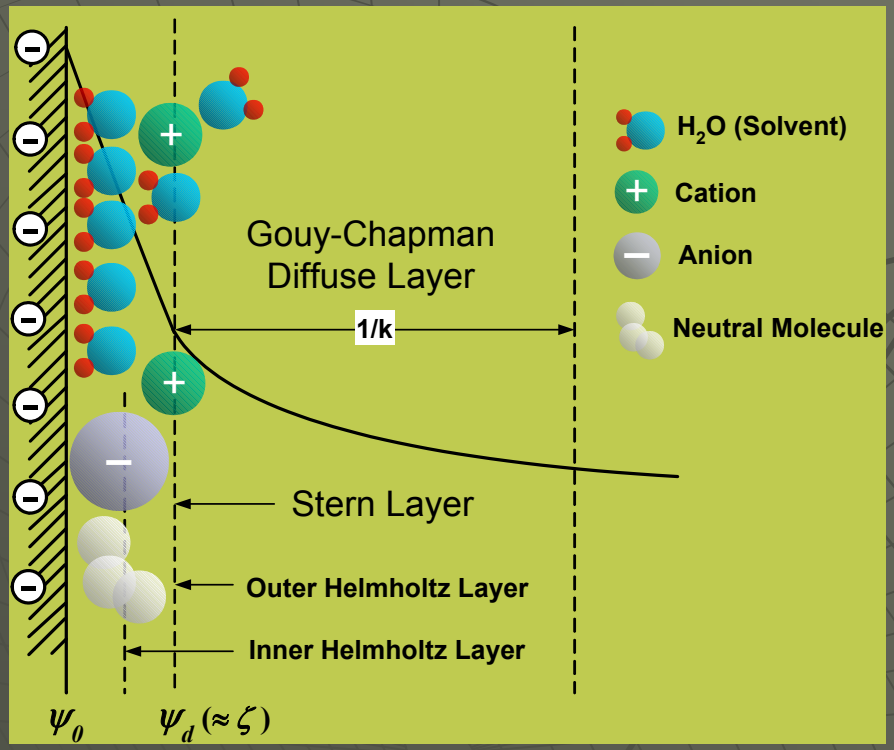

$$\psi = \frac{2k_B T}{ze} \ln\left(\frac{1+\gamma\exp(-\kappa x)}{1-\gamma\exp(-\kappa x)}\right)$$

$$\gamma = \tanh\left(\frac{ze\varphi_o}{4k_B T}\right)$$

$$\sigma = (8k_B T c_o^* \varepsilon_o \varepsilon_r)^{1/2} \sinh\left(\frac{ze\varphi_o}{2k_B T}\right)$$

K_B : Boltzmann constant
φ_0 : Potential at (x=0)
z : Ion valency
x : Distance from the surface
T : Temperature
ε_o : Permittivity of free space
ε_r : Solvent dielectric constant
C_o : Electrolyte concentration

Non-Faradaic : No electron transfer

Ex) Dielectric Capacitor
Electric Double Layer Capacitor

Pseudocapacitance

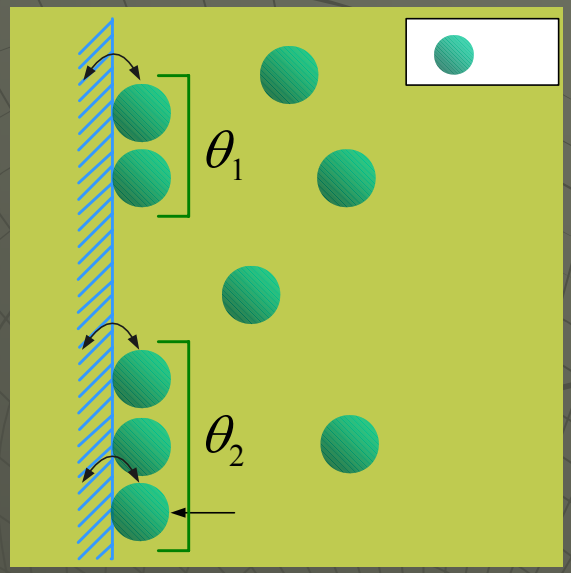

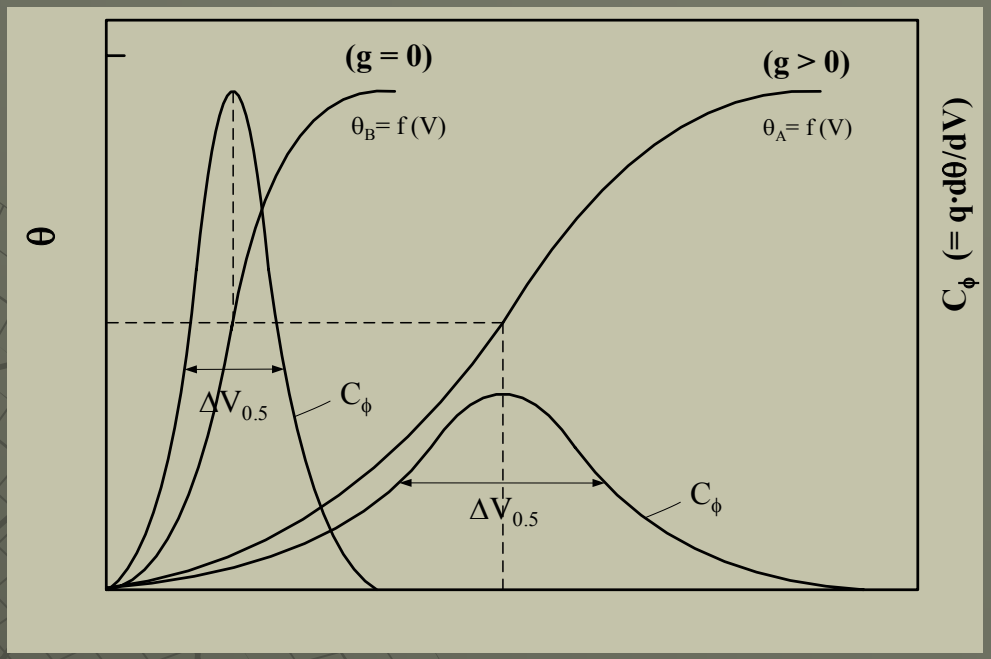

$$Ox + ze \leftrightarrow \mathrm{Re}\,d$$

Faradaic : electron transfer

Ex) Battery, Pseudocapacitor

θ : Coverage
V : Voltage
K : Reaction rate constant
g : Adsorption isotherm constant
F : Faraday constant

e^-

$$\frac{\theta}{1-\theta} = K \exp\left[\frac{VF}{RT}\right] \exp(\pm g\theta)$$

$$C_\phi \approx \frac{d\theta}{dV} = \frac{F}{RT} \cdot \frac{K \exp\left[\frac{VF}{RT}\right]}{\left(1 + K \exp\left[\frac{VF}{RT}\right]\right)^2}$$

Φ

Competitive Systems

	Material	Gravimetric Capacitance (F/g)	Electrolyte	Potential Window (V)	Scan rate (mV/s)	Reference
Carbon	Multi-walled carbon nano-tubes	113	38wt% H_2SO_4	0	-	Niu *et al.*
	Carbon nano-tubes	15 ~ 25	38wt% H_2SO_4	0 – 0.9	10mA	Ma *et al.*
	Mesoporous Carbon	95	1M $LiPF_6$	0.75 – 3.75	5	Zhou *et al.*
Transition Metal Oxide	RuO_2	350	0.5M H_2SO_4	0 – 1	100	Raistrick *et al.*
	$RuO_2 \cdot xH_2O$	720 ~ 760 250	0.5M H_2SO_4	0 – 1	2 50	Zheng *et al.*
	RuO_2 on Carbon Tape	900	0.5M H_2SO_4	0.2 – 0.7	2	Long *et al.*
	Amorphous $MnO_2 \cdot H_2O$	153	1M KCl	0.1 – 0.85	10	Lee *et al.*
	NiO_x	260	1M KOH	-0.4 – 0.5	10	Liu *et al.*
	$Co(OH)_2$ Xerogel	291	1M KOH	-1.1 – 0.8	50	Lin *et al.*
	Fe_3O_4	38	1M Na_2SO_4	-1.2 – 1.2	2	Wu *et al.*
Polymer	Poly3-(3,5-difluorophenylthiophene)	23 ~ 30mAh/g	Poly(acrylonitrile)	-2 – 0	25	Searson *et al.*
	Poly(dithienothiophene)-pDTT	15	Poly(ethylene oxide) – PEO	0 – 0.3	50	Arbizzani *et al.*
	Polyaniline (PANI)	25	Poly(methylmethacrylate) – PMMA	0 – 1.2	50	Clement *et al.*
	Polyaniline (PANI) on Stainless Steel	650~1300	1M $LiClO_4$ in PC	0 – 0.75	200	Prasad *et al.*

Transition Metal Nitrides: Novel Capacitor Materials

- Good Electrical Conductivity
  - High rate electrochemical response of the capacitor depends on electrical conductivity of the electrode and the ionic conductivity of the electrolyte
- Chemical Stability
  - The electrolyte widely used are corrosive (H_2SO_4 or KOH)
- Cost
- High Mass Density (g/cm^3)
  - To increase volumetric capacitance (F/cc)
- High Specific Surface Area (m^2/g)
  - To increase the electrode-electrolyte interface area for charge storage

Physical Properties of Materials

Material	Structure	Density (g/cm^3)	Electronic Conductivity $\sigma \times 10^{-2} \Omega^{-1} m^{-1}$	M.W.
RuO_2	Tetragonal ($P4_2/mnm$)	6.97	2×10^6	133.07
Carbon	-	< 1	$< 4 \times 10^4$	12.00
TiN	Cubic (Fm3m)	5.43	2.5×10^4	61.91
VN	Cubic (Fm3m)	6.04	1.67×10^4	64.95
ZrN	Cubic (Fm3m)	7.09	5.55×10^4	105.23
NbN	Cubic (Fm3m)	8.3	1.28×10^4	106.91
Mo_2N	Cubic (Pm3m)	8.4	5.05×10^4	205.88
TaN	Cubic (Fm3m)	14.1	5.55×10^4	194.96
Ta_3N_5	Orthorhombic (Cmcm)	—	$< 10^{-4}$	612.87
WN	Cubic (Pn3m)	12.12	—	197.89

Ref: 1) J. P. Zheng, P. J. Cygan, and T. R. Jow, *J. Electrochem. Soc.*, 142(8), (1995) p.2699
2) M. Wixom, L. Owens, J. Parker, J. Lee, I. Song, and L. Thompson, *Electrochem. Soc. Proc.,* 96 (25) (1999) p. 63
3) P. T. Shaffer, *Handbook of High-Temperature Materials*, Vol.1, pp.292-92. Plenum Press, New York, (1964)

TEM Analysis: Morphology of the Nanocrystalline Nitirdes

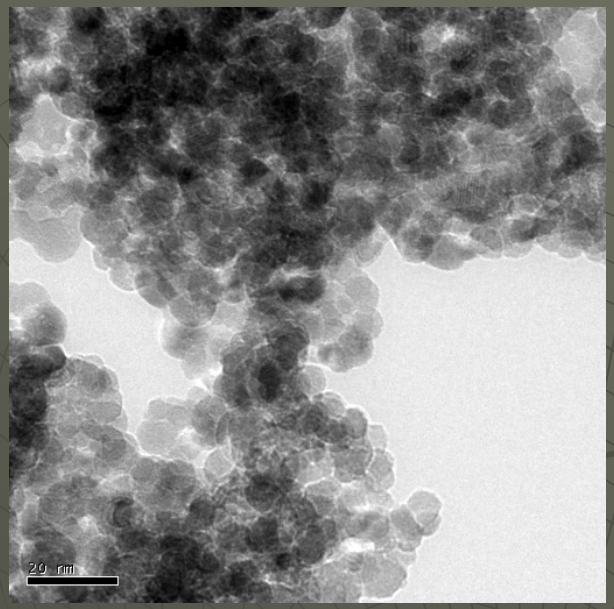

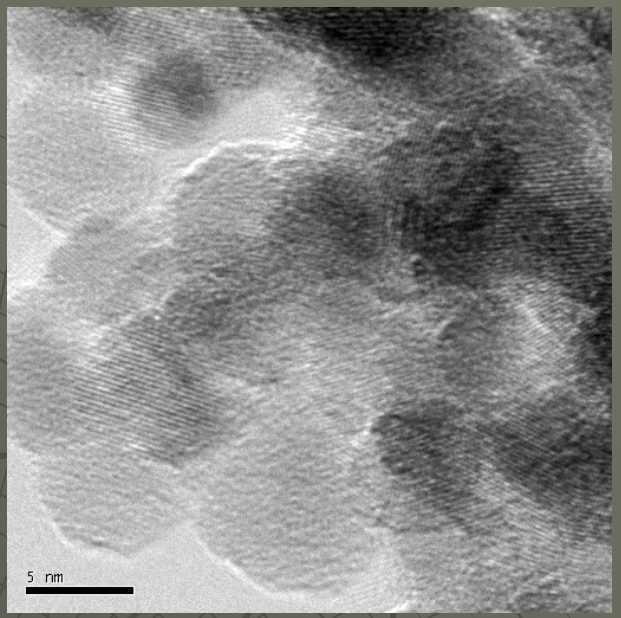

VN500^{o} C

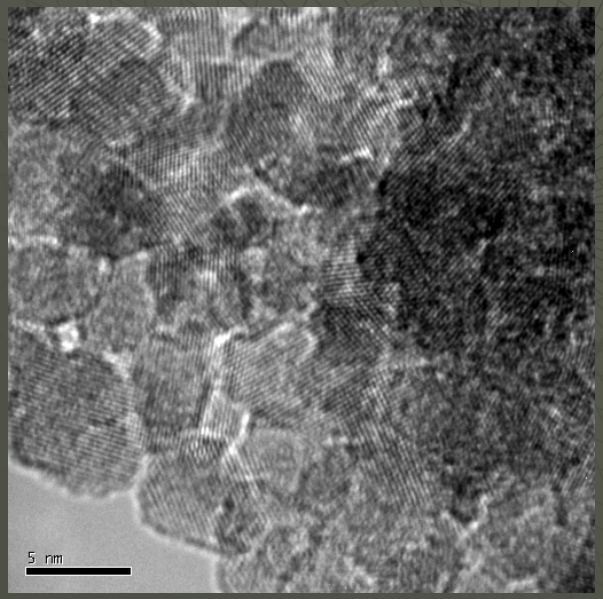

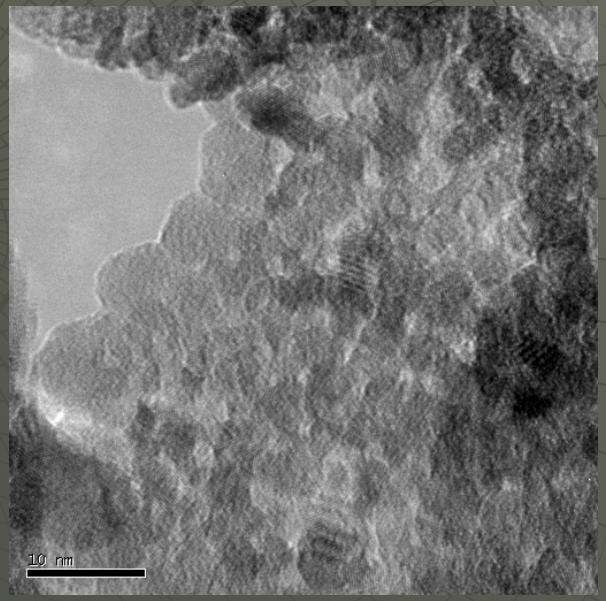

VN-400°C

Electrochemical Response of the Nanocrystalline Nitrides

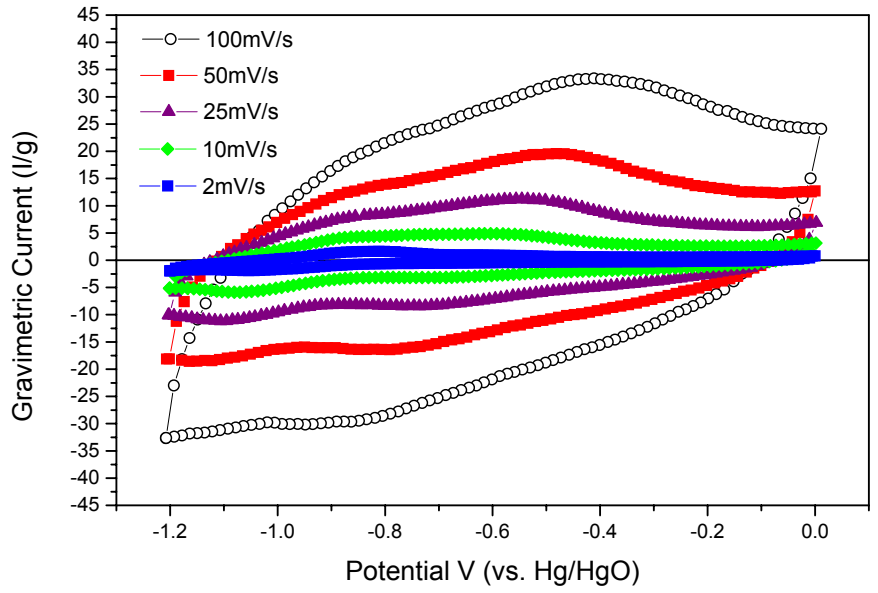

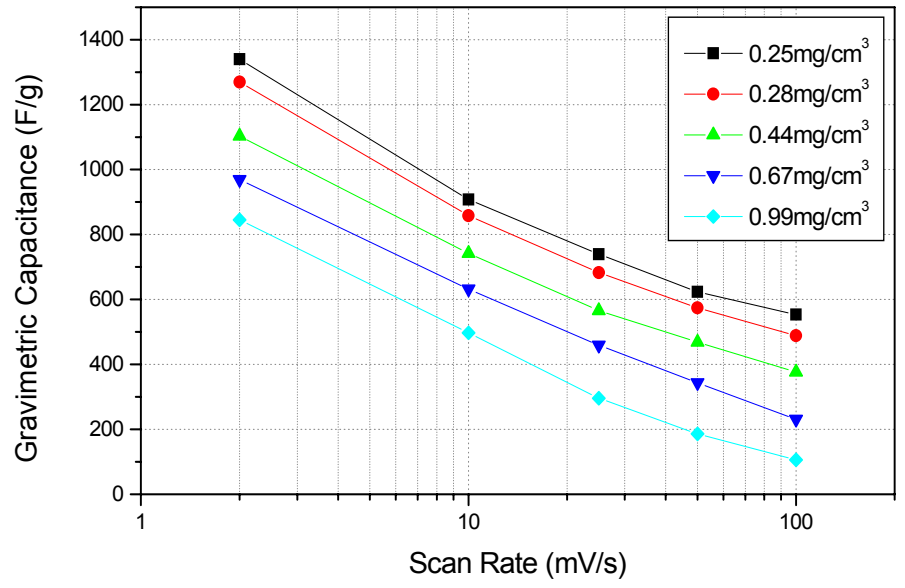

Figure 2 The (a) cyclic voltammogram of nanocrystallites synthesized at 400°C and (b) gravimetric capacitance (F/g) versus VN nanocrystallites loading scanned at various rates (2~100mV/s) in 1M KOH electrolyte.

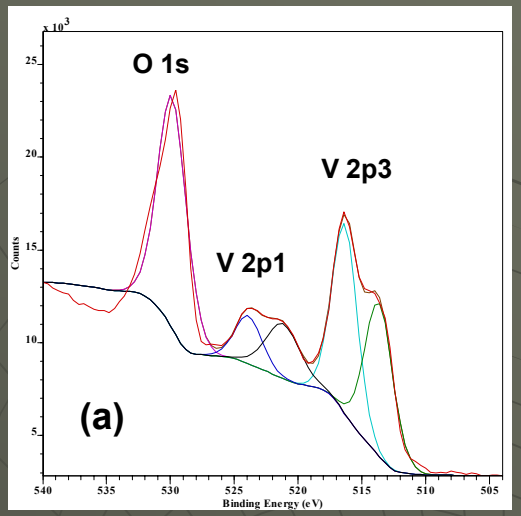

XPS: Presence of V_2O_5 before cycling

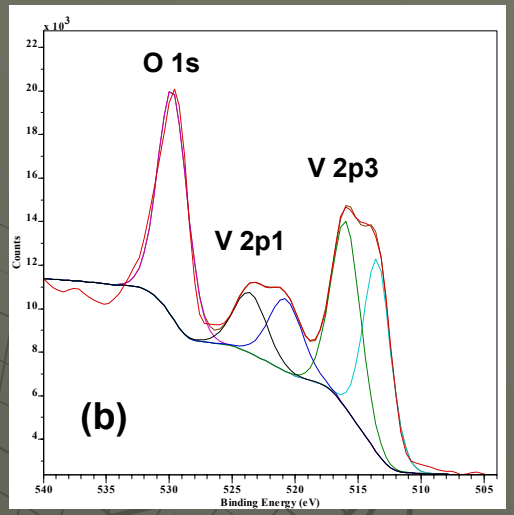

XPS: Formation of V_2O_3 after 200 cycles

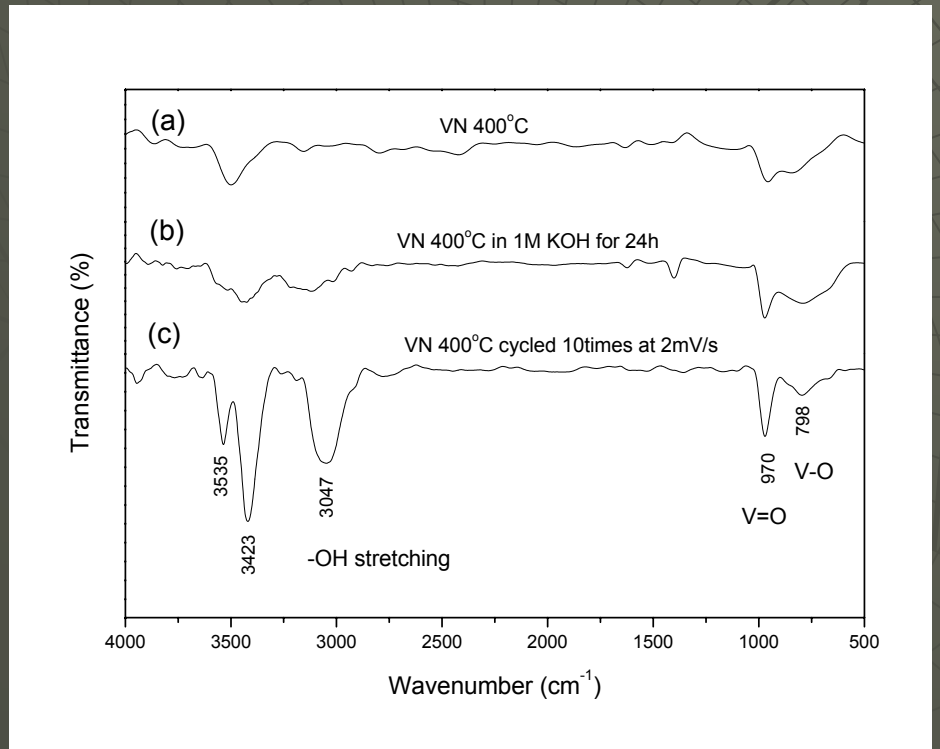

The FTIR spectra of (a) VN powder, immersed in 1M KOH solution for 24h and cycled 200 times and XPS spectra of VN powder (b) before and (c) after electrochemically cycled for 200 times.

Controlled oxidation is the key minimal reduction in electronic conductivity

Major Benefits of Direct Methanol Fuel Cells

- **High Efficiency of Energy Conversion**
  - Enhanced utilization of fuel
  - Lower carbon dioxide emissions
- **Direct Generation of Electrical Energy**
  - Losses in mechanical to electrical energy conversion is avoided
- **Low temperature operation**
  - Low emissions of nitrogen oxides, carbon monoxide and particulates

Potential solution for portable applications

- Near Ambient temperature operation
- High energy density required
- Easy to handle fuel

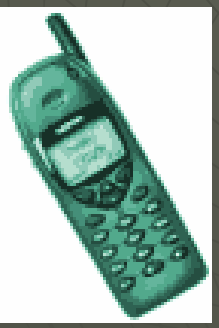

2W

20W

50-100W

500W

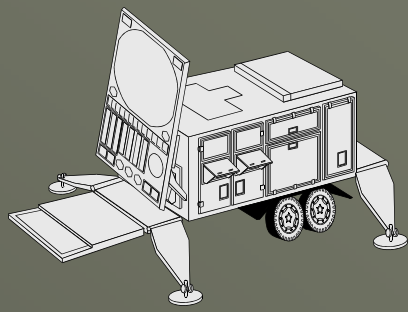

1-5kW

DIRECT METHANOL FUEL CELL SYSTEM

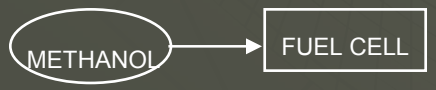

CO_2 Emissions and Efficiency for Traditional ICE and methanol or hydrogen fed Fuel Cells

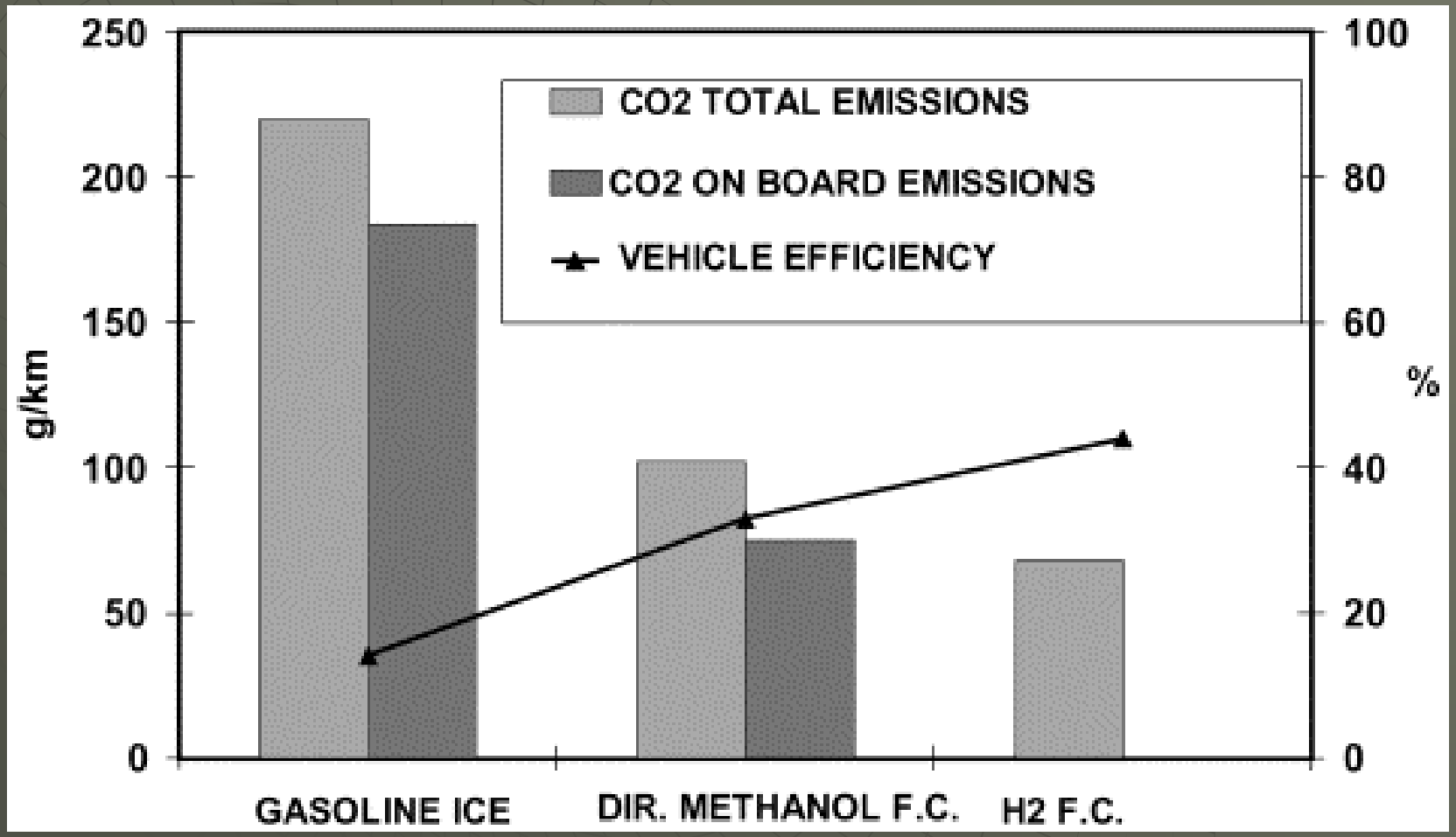

G. Cacciola *et al.* J. Power Sources 100 (2001) 67-79

Drawbacks

- Expensive materials
  - Platinum catalysts, fluoropolymers
- Components that are expensive to manufacture
- Lack of fuel flexibility
- Requires clean fuel; *e.g.* sulfur free
- Electrochemical reactions are sensitive to poisons in the environment

Direct Methanol Fuel Cell Concept

Anode (Pt-Ru)

$CH_3OH + H_2O \longrightarrow CO_2 + 6H^+ + 6e^-$

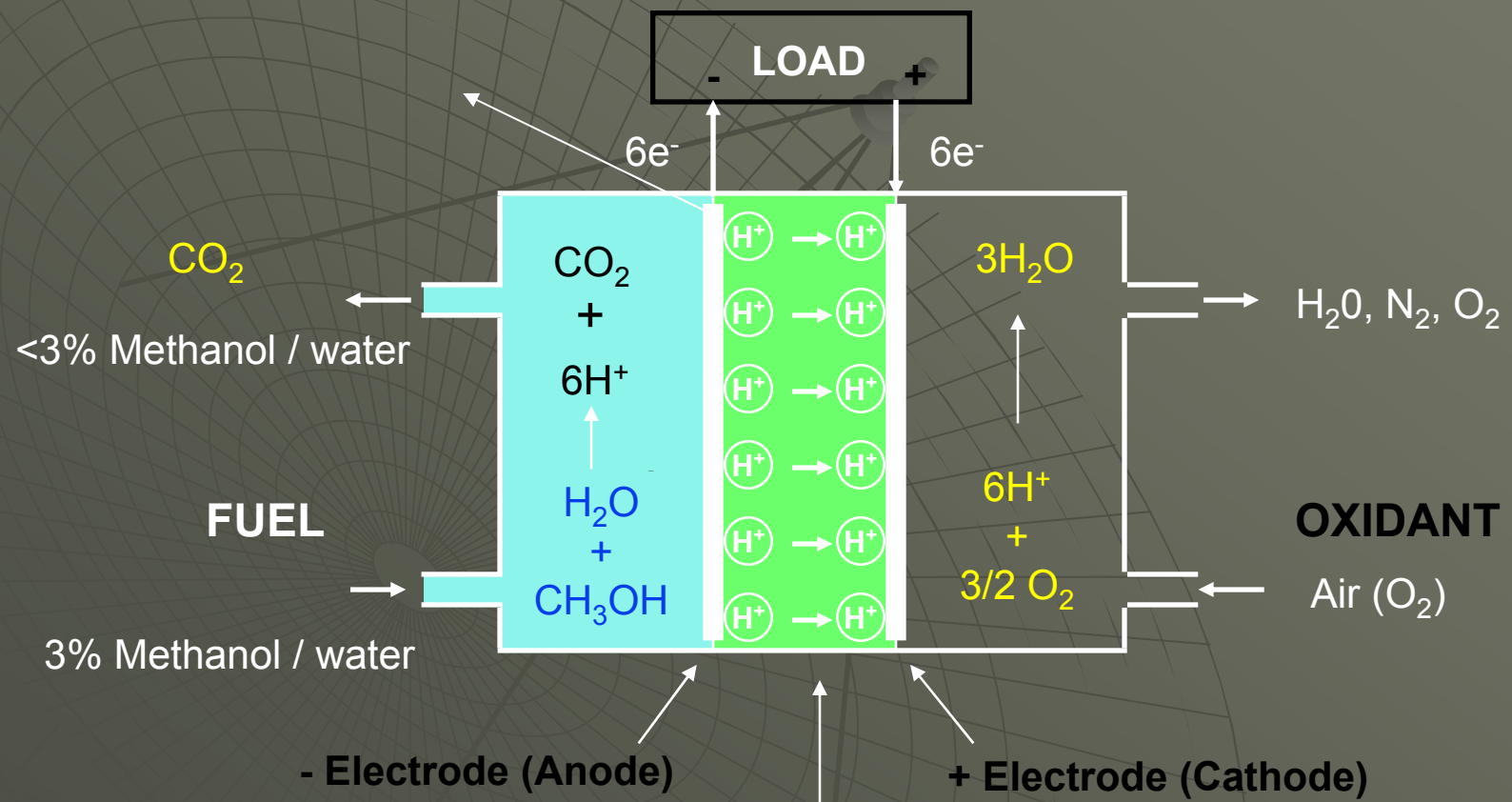

Cathode (Pt)

$6H^+ + 1.5\ O_2 + 6e^- \longrightarrow 3H_2O$

Synthesis of Catalysts

- Most synthetic approaches in the literature are based on the reduction of Halide precursors of Pt and Ru
- Limitations:

  —Need for several washing steps to eliminate unwanted by-products

  —Tedious process leading to loss of active material

  — Poisoning of the catalyst
- Need for improved catalyst using non-halogen containing precursors
- Objective: Develop novel sol-gel based methods using non-halogen precursors for generating Pt-Ru catalysts
  - High surface area
  - Pt to Ru ratio close to unity
  - High electrochemical activity
  - (low polarization of the electrode)

Morphology Characterization *Transmission Electron Microscopy (TEM)*

- TEM micrographs of the powder possessing the highest surface area (120-160 m^2/g) with the best electrochemical activity (optimized sample)

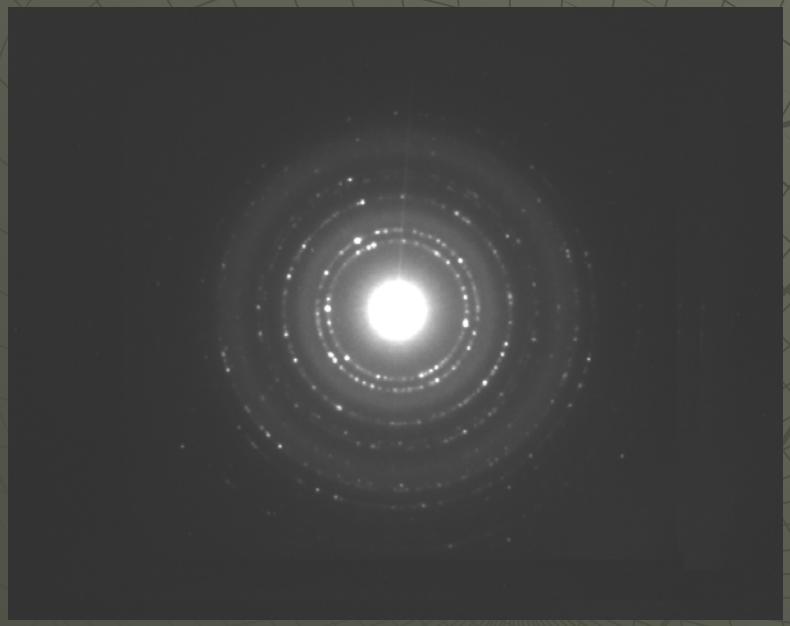

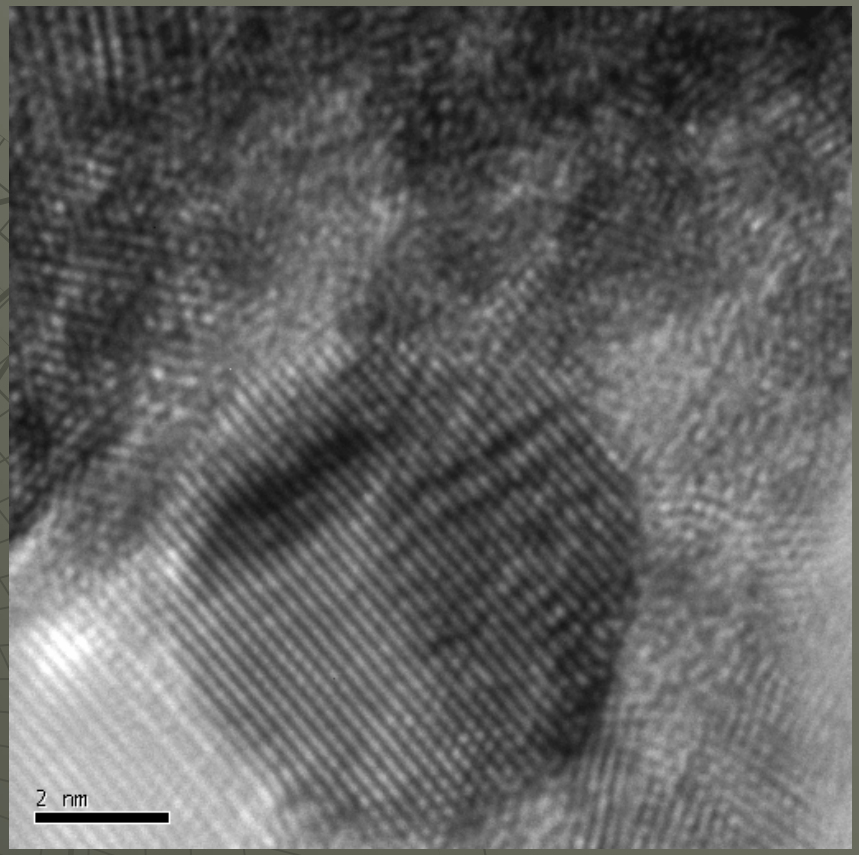

—Diffraction pattern indicates single phase Pt-Ru composition

—HRTEM images show 2-4 nm sized crystallites

Electrochemical Characterization
Anode polarization data

•Results of electrochemical tests conducted on the powders derived using a large excess of tetramethylammonium hydroxide [TMAH : (Pt-acac+Ru-acac) = 1.75:1 and Pt:Ru = 1:1]

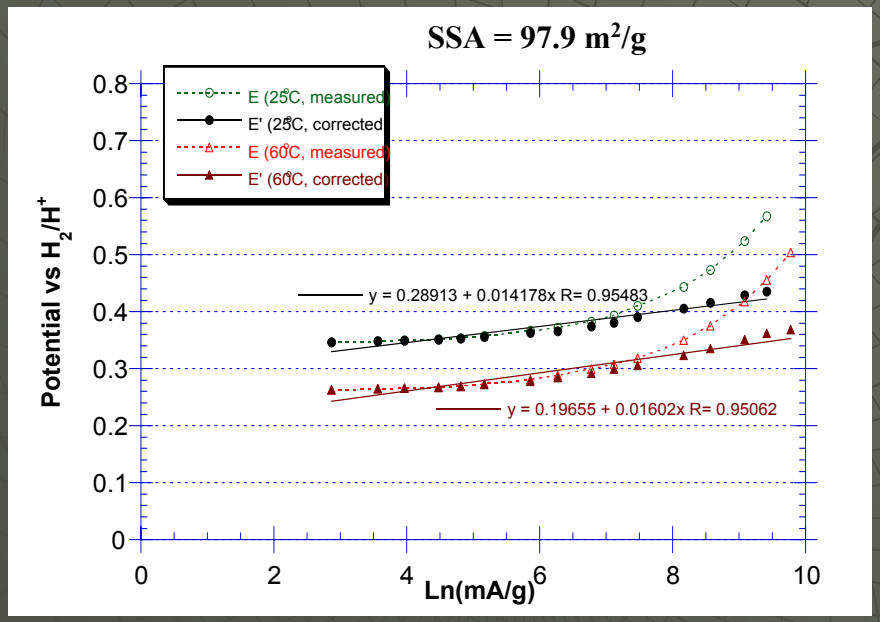

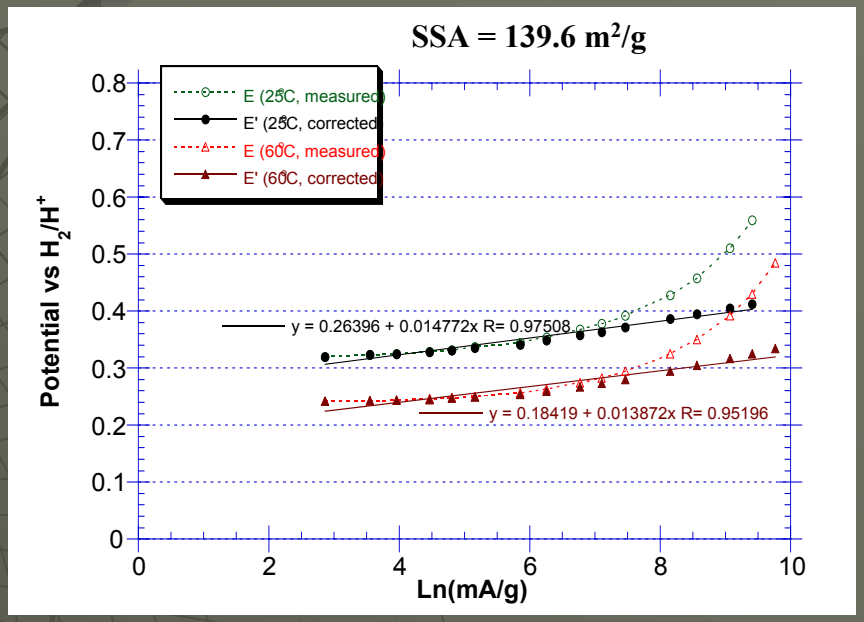

(a) Two step heat treatment of

400/3h/1%O_2 (3 g) → (0.5g)300/3h/1%O_2

IV-1-1

(b) Two step heat treatment of

300/2h/1%O_2 (3 g) → (0/5g)300/4h/1%O_2

IV-1-2

Comparison of catalytic activity

Sample	Specific surface area (m^2/g)	Intercept on y axis in polarization curve		Slope in polarization curve		Cell potential (V) at ln(mA/g)=8 (60°C)	
		25°C	60°C	25°C	60°C		
JPL	**49.5**	**0.305**	**0.182**	**0.0216**	**0.0193**	**0.336**	
Giner	**94.2**	**0.269**	**0.177**	**0.0273**	**0.0306**	**0.422**	
Johnson-Matthey	**71.3**	**0.298**	**0.173**	**0.0127**	**0.0163**	**0.304**	
1208.12	94.2	0.214	0.155	0.0284	0.0231	0.340	TMAH:acac=1.25:1 Pt:Ru = 1:1
1212.03	95.9	0.322	0.217	0.0169	0.0194	0.372	TMAH:acac=1.25:1 Pt:Ru = 1:1.25
1214.03	97.9	0.289	0.197	0.0142	0.0160	0.325	TMAH:acac=1.25:1 Pt:Ru = 1:1.5
1214.10	**139.6**	**0.264**	**0.184**	**0.0148**	**0.0139**	**0.295**	**TMAH:acac=1.75:1 Pt:Ru = 1:1**

Sample identification	Surface area(m^2/g)	Phase/phases present	Lattice parameter (nm)	Carbon content (%)
JM catalyst	70	Pt(Ru)	0.3866	0
JM catalyst-(600°C/6h in Ar)	-	Pt(Ru) +Ru	0.3858	0
Sample A (500^{0}C/6h in Ar)	1	Pt(Ru) + C	0.3861	63
Sample B (Sample A: 300^{0}C/2h in Ar-1% O2)	158	Pt(Ru) + C	0.3859	3
Sample C (Sample B: 300^{0}C/2h in Ar-1% O_2)	120	Pt(Ru)	0.3859	0

Prospects for Future

- Nanomaterials show potential for energy storage
- Nanoscale phenomena in batteries, fuel cells and supercapacitors still need to be studied
- Considerable potential for integration, theoretical and experimental studies